Local structure evolution of $Fe_xNi_{77-x}Cu_1Nb_2P_{14}B_6$ soft magnetic materials by mechanical alloying

Shilong Yin[a], Shiqiang Wei[b]*, Qing Bian[c], and Zhongrui Li[b]

[a]Department of Mathematics and Physics, Hohai University, Nanjing, 210024. P.R.China.
[b]National Synchrotron Radiation Laboratory, University of Science and Technology of China, Hefei 230029 P.R.China.
[c]Department of Basic Science, Institute of Communication Engineering, Nanjing, 210016 P.R.China,
E-mail: sqwei@ustc.edu.cn

Mechanically alloyed $Fe_xNi_{77-x}Cu_1Nb_2P_{14}B_6$ soft magnetic materials have been prepared with different atomic compositions. The alloy structures are investigated by X-ray absorption fine structure (XAFS). The results show that mechanical alloying (MA) can drive the $Fe_xNi_{77-x}Cu_1Nb_2P_{14}B_6$ powder mixture to produce amorphous alloy while the atomic concentration of Fe element is about and over 40%. On the contrary, the MA $Fe_xNi_{77-x}Cu_1Nb_2P_{14}B_6$ is a solid solution with a fcc-like structure in the region of lower Fe atomic concentration (<22%), preserving a medium-range order around Ni and Fe atoms. Moreover, we have found that the local structure geometry of Fe atom is similar to that of Ni atom for all the MA $Fe_xNi_{77-x}Cu_1Nb_2P_{14}B_6$ samples. It indicates that the local structures of Fe and Ni atoms in a $Fe_xNi_{77-x}Cu_1Nb_2P_{14}B_6$ sample only depend on the x value of element Ni after ball milling.

Keywords: XAFS; local structure; soft magnetic materials; mechanical alloying.

1. Introduction

Recently, more and more effort has been devoted to search some better soft magnetic materials that not only possess high magnetic permeability and low coercive force but also have high saturation flux density in high magnetic field (Inoue *et al*., 1998; Idzikowski *et al.*, 1998; Fragman *et al*., 1998). The Fe-based amorphous alloys are promising materials with good soft magnetic properties. Yoshizawa *et al.* (1998) have found that a homogeneous, nanocrystalline phase of α-Fe(Si) with typical grain diameter of 10~15 nm was present in the amorphous Fe-Si-B-M (M: Cu, Nb, Mo, W, Ta, etc) alloy ribbon after thermal annealing. The nanocrystalline Fe-Si-B-M alloy exhibits higher value of saturation magnetization and permeability as compared with those of conventional Fe-Cu-Nb-Si-B alloys (Hezer, 1992). More recently, we have found that $Fe_xNi_{77-x}Cu_1Nb_2P_{14}B_6$ amorphous soft magnetic materials can be produced by mechanical alloying (MA), and their properties were greatly influenced by the atomic concentration x of element Fe. In order to explain the magnetic properties of the MA alloys, it is very important to determine the local structures around Fe and Ni atoms (Wu *et al.*, 1999; Chen *et al.*, 1999; Eric *et al.*, 1999).

In this work, X-ray absorption fine structure (XAFS) was employed to investigate the effect of Ni content on the local structures of Fe and Ni atoms in $Fe_xNi_{77-x}Cu_1Nb_2P_{14}B_6$ sample. A metastable solid solution with fcc-like structure was observed for the MA $Fe_xNi_{77-x}Cu_1Nb_2P_{14}B_6$ soft magnetic materials in the region of a lower Fe concentration. In contrast, an amorphous alloy was produced for MA $Fe_xNi_{77-x}Cu_1Nb_2P_{14}B_6$ soft magnetic materials in the region of a higher Fe concentration (> 40%). This result indicates that the property and structure of $Fe_xNi_{77-x}Cu_1Nb_2P_{14}B_6$ soft magnetic materials are easily controlled by the atomic concentration of Ni.

2. Experimental

The precursor materials, Fe, Ni, Cu, Nb, P and B powders with the composition of $Fe_xNi_{77-x}Cu_1Nb_2P_{14}B_6$ were mixed together, and then the mixture and tungsten carbide balls were sealed inside a cylindrical stainless steel vial filled with argon gas. The weight ratio of the balls to the powder was 40:1. MA was performed in a planetary ball mill with a rotation speed of about 210 r/min and the milling time of 120 hours. The XAFS spectra of the Fe and Ni K-edges were measured at the U7C beam-line of National Synchrotron Radiation Laboratory (NSRL) and the 4W1B beam-line of Beijing Synchrotron Radiation Facility (BSRF). The monochromator is two flat Si (111) crystals with a fixed exit. Data were collected in transmission mode at room temperature. The XAFS data were analyzed by USTCXAFS1.0 software package (Wan, *et al.*, 1999). The results display that the experiment deviation of the main peak intensity of radial distribution curve obtained from NSRL and BSRF was within 3% for a sample.

3. Results and discussions

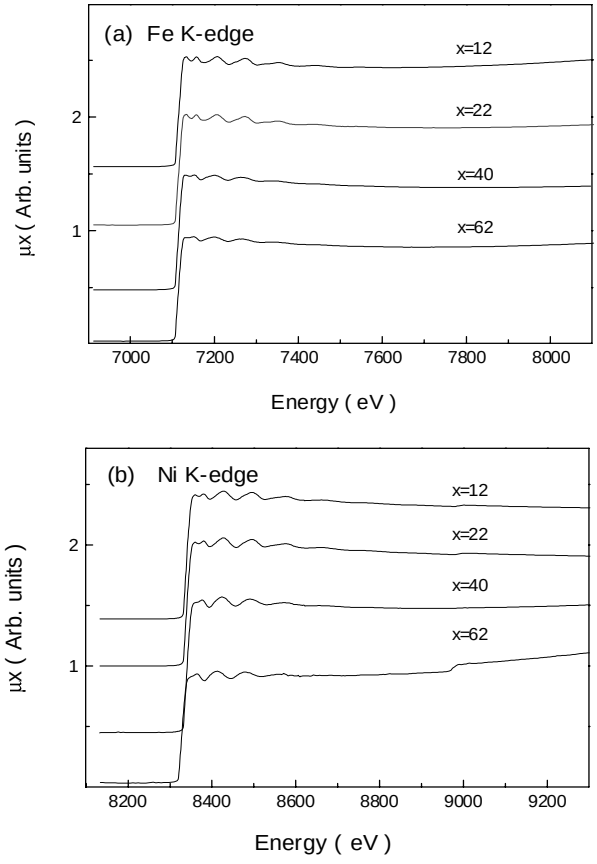

Figure 1
Fe and Ni K-edge XAFS spectra of $Fe_xNi_{77-x}Cu_1Nb_2P_{14}B_6$ alloys

The XAFS spectra of Fe and Ni K-edge of $Fe_xNi_{77-x}Cu_1Nb_2P_{14}B_6$ alloys were shown in Figure 1 (a) and (b). It can be observed that the magnitude of the oscillation peak strongly decreases with the increase of Fe content. Particularly, the large difference occurs at the x value between 40 and 22. There are six oscillation peaks in the range of 400 eV above the Fe and Ni K-edge for the MA $Fe_{12}Ni_{65}Cu_1Nb_2P_{14}B_6$ and $Fe_{22}Ni_{55}Cu_1Nb_2P_{14}B_6$. However, only four weak oscillation peaks can be found in the region of 400 eV beyond Fe and Ni K-edge for $Fe_{62}Ni_{15}Cu_1Nb_2P_{14}B_6$ and $Fe_{40}Ni_{37}Cu_1Nb_2P_{14}B_6$. The result indicates that the disorder degree around Fe and Ni atoms significantly increases after the MA while the Fe atomic concentration is about and over 40%.

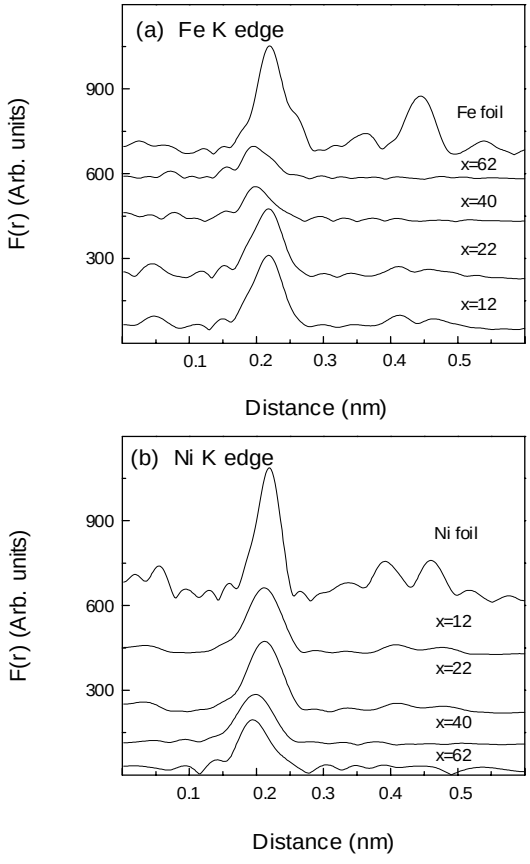

Figure 2
Radial distribution curves of Fe (a) and Ni (b) atoms in $Fe_xNi_{77-x}Cu_1Nb_2P_{14}B_6$ alloys

The results of Fourier transformation of EXAFS oscillation function $k^3\chi(k)$ (k_{min}=25 nm^{-1}, k_{max}=160 nm^{-1}) for samples representing the radial distribution curves F(r) are displayed in Figure 2 (a) and (b). A different feature is easily found from the curves of bcc structure Fe foil and fcc structure Ni foil. A stronger amplitude peak responding to the fourth coordination shell appears at 0.444 nm for bcc Fe, but two weaker amplitude peaks of the third and fourth coordination shell emerge at 0.396 and 0.46 nm for fcc Ni, respectively. The shapes of radial distribution curves of Fe and Ni powders are similar to those of their foils, except for the intensity being a little lower. However, the radial distribution curves of Fe atoms in the MA $Fe_{62}Ni_{15}Cu_1Nb_2P_{14}B_6$ and $Fe_{40}Ni_{37}Cu_1Nb_2P_{14}B_6$ show that only the main amplitude peak can be observed and the higher distance amplitude peak fully disappears. Furthermore, the first peak intensity decreases by three times as well as the position of the first peak contracts by 0.020 nm when Fe atomic concentration is beyond 40%. The ultrafine Fe-Ni alloy particle for Fe rich phase is tended to form amorphous metastable phase with element P and B just as the conclusions of Liu *et al.* (1999) and Garciaarribas *et al*. (1999).

Table 1
Local structure parameters of Fe atoms from XAFS data of $Fe_xNi_{77-x}Cu_1Nb_2P_{14}B_6$ sample

Sample (x%)	Bond type	R_j (nm)	R_0 (nm)	σ_T (nm)	σ_s (nm)	N	$\bullet E_0$ eV
Fe foil	Fe-Fe	0.248				8.0	
62	Fe-M[#]	0.272	0.240	0.0075	0.032	10.6	0.9
40	Fe-M	0.265	0.241	0.0075	0.025	10.5	1.6
22	Fe-M	0.250	0.244	0.0076	0.006	11.0	1.5
12	Fe-M	0.249	0.244	0.0074	0.005	11.4	2.0

[#] M=Fe, Ni; Errors of R_j, R_0,σ_T, σ_S and N are ±0.002 nm, ±0.002 nm, ±0.0005 nm and ±0.8, respectively.

Table 2
Local structure parameters of Ni atoms from XAFS data of $Fe_xNi_{77-x}Cu_1Nb_2P_{14}B_6$ sample

Sample (x%)	Bond Type	R_i (nm)	R_0 (nm)	σ_T (nm)	σ_s (nm)	N	$\bullet E_0$ eV
62	Ni-M[#]	0.262	0.239	0.0079	0.023	10.8	3.0
40	Ni-M	0.260	0.240	0.0080	0.020	11.0	4.0
22	Ni-M	0.253	0.245	0.0078	0.008	11.5	1.0
12	Ni-M	0.251	0.246	0.0075	0.005	11.2	0.5
Ni foil	Ni-Ni	0.249				12.0	

[#] M and errors are the same as those in Table 1

In order to obtain the local structure parameters of Fe and Ni atoms in the MA $Fe_xNi_{77-x}Cu_1Nb_2P_{14}B_6$ alloys, the convolution of Gaussian function P_G and exponential function P_E was used to describe the asymmetric atom distribution function around Fe and Ni atoms for these disorder system (Wei *et al*., 2000; Sayers *et al*., 1988). The fitting results of the sample (x=40) show that the average bond length R, closed packing bond length R_0 ($R=R_0+\sigma_S$), the coordination number N around Fe atom, thermal disorder factor σ_T and static disorder factor σ_S are 0.265±0.002 nm, 0.241±0.002 nm, 10.5±0.8, 0.0075±0.0005 nm and 0.025±0.0005 nm, respectively. The structural parameters indicate that the average bond length R_{Fe-M} (0.265 nm) for the first coordination shell of Fe atom in the MA $Fe_{40}Ni_{37}Cu_1Nb_2P_{14}B_6$, is about 0.017 nm larger than that of Fe foil (R=0.248 nm) or Ni foil (R=0.249 nm). The σ_S value is about 3.5 times as large as the σ_T. The results imply that there is an amorphous character around the Fe atoms in the MA $Fe_{40}Ni_{37}Cu_1Nb_2P_{14}B_6$. In contrast, the local structures of Fe atoms in the MA $Fe_{22}Ni_{55}Cu_1Nb_2P_{14}B_6$ and $Fe_{12}Ni_{65}Cu_1Nb_2P_{14}B_6$ are evidently different from that of the MA $Fe_{40}Ni_{37}Cu_1Nb_2P_{14}B_6$. No bond length R contracts for the MA $Fe_{22}Ni_{55}Cu_1Nb_2P_{14}B_6$ as shown in Figure 2 (a). On the other hand, we have noted that the stronger peak located at about 0.444 nm disappears, while the two

weak peaks located at 0.396 nm and 0.46 nm appear in the radial distribution curve of Fe atom for $Fe_{22}Ni_{55}Cu_1Nb_2P_{14}B_6$ and $Fe_{12}Ni_{65}Cu_1Nb_2P_{14}B_6$ samples. Two different interpretations are postulated. In the first case, Fe atoms are incorporated into the fcc-lattice of Ni because of large surface area in $Fe_{22}Ni_{55}Cu_1Nb_2P_{14}B_6$ and $Fe_{12}Ni_{65}Cu_1Nb_2P_{14}B_6$ samples. In the second interpretation, the bcc-lattice of Fe undergoes a first-order phase transition from bcc-like coordination to fcc-like dense packing as the internal pressure surpass a critical pressure. In the former case, the Fe-Ni alloying is achieved while in the latter case, they form the separated Fe and Ni clusters. If all Fe atoms were incorporated into a fcc Ni lattice, the Ni atoms is expected to have a large distortion which would appear as a sharp drop of the Ni main FT peak intensity. Since we find that the Ni local structure is not changed during MA, the interpretation of Fe atoms incorporating into the fcc-lattice of Ni is unlikely. It reveals clearly that the MA can drive the local structure of Fe atom in the MA $Fe_{22}Ni_{55}Cu_1Nb_2P_{14}B_6$ sample to change from the initial bcc structure into the final fcc structure. The fitting results of the sample (x=12) show that R, R_0, N, σ_T and σ_S are 0.251±0.002 nm, 0.246±0.002 nm, 11.2±0.8, 0.0075±0.0005 nm and 0.0050± 0.0005 nm, respectively. The average bond length R (0.251 nm) and the coordination number N (11.2) are well identical to those of fcc structure Ni foil (R=0.249 nm, N=12). The XAFS result of $Fe_{22}Ni_{55}Cu_1Nb_2P_{14}B_6$ seems to suggest that the element Fe and Ni have formed fcc structural Fe-Ni solid solution during the MA process. From viewpoints of internal pressure or stress, a small grain size is advantageous for phase change. In the previous study, We have reported that the MA can drive the bcc structural Fe and fcc structural Cu in a Fe and Cu powder mixture to form nanocrystalline solid solution with the fcc structure (Wei *et al.*, 1997). The radial distribution curves obtained from Ni XAFS spectra were demonstrated in Figure 2 (b). We found that the local structure geometry of Ni atoms is the same as that of Fe atoms in the MA $Fe_xNi_{77-x}Cu_1Nb_2P_{14}B_6$ sample. As long as the local structure of Fe atoms in the MA $Fe_{40}Ni_{37}Cu_1Nb_2P_{14}B_6$ is amorphous, the local structure of Ni atoms in this sample is amorphous too. If the Ni atoms in the MA $Fe_{22}Ni_{55}Cu_1Nb_2P_{14}B_6$ keep fcc structure with a medium-range order, the local structure of Fe atoms is changed from bcc into fcc structure and the solid solution is formed.

4. Conclusions

The XAFS results of Fe and Ni atoms in the MA $Fe_xNi_{77-x}Cu_1Nb_2P_{14}B_6$ samples have clearly showed that after ball milling the bcc structure α-Fe and fcc structure Ni disappear while the atomic concentration of Fe element is about and over 40%. It means that the MA can drive $Fe_{40}Ni_{37}Cu_1Nb_2P_{14}B_6$ or $Fe_{62}Ni_{15}Cu_1Nb_2P_{14}B_6$ mixtures to form amorphous alloys. With the x value (Fe concentration) decreasing, the local structures around Fe and Ni atoms possess fcc structural geometry with a medium-range order for the MA $Fe_{22}Ni_{55}Cu_1Nb_2P_{14}B_6$ and $P_{14}B_6$ samples. Therefore, we consider that in the lower Fe $Fe_{12}Ni_{65}Cu_1Nb_2$ concentration region (smaller than 22%), elements Fe and Ni are preferred to produce fcc-like Fe-Ni solid solution during the MA process. The Fe-Ni solid solution for Ni rich phase is difficult to further form amorphous alloy with element P and B by MA. In the higher Fe concentration region (> 40%), the Fe-Ni alloy for Fe rich phase is tended to form amorphous metastable phase with element P and B after milling for 120 hours. These results indicate that the structure of the MA product can be controlled by the composition of Fe_xNi_{77-x} $Cu_1Nb_2P_{14}B_6$ mixture. It opens a new way for preparing $Fe_xNi_{77-x}Cu_1Nb_2P_{14}B_6$ soft magnetic materials with nice performances by using the MA method.

Acknowledgements

This research work is supported by the " 100 people plan" and "95 programs" of Chinese Academy of Sciences. We would like to thank National Synchrotron Radiation Laboratory and Beijing Synchrotron Radiation Facility for giving us the beam time for XAFS measurement.

References

Chen, X.L, Lan, Y.C., Liang, J.K., Cheng, X.R., Xu, Y.P., Xu, T., Jiang, P.Z., & Lu, K.Q. (1999). *Chin. Phys. Lett.* **16(2),** 107.

Eric, G., Frederic, B., Niepce, J.C., Frederic, C., Christophe, G., Gerard,L.C., Guichard, J.L., Pierre, D., Alain M. & Olivier, T.(1999). *J. Mater. Chem.* **9,** 305.

Frayman, L.I., Ryan, D.R., & Ryan ,J.B. (1998). *International of Powder Metallurgy,* **34**, 7.

Garciaarribas A., Fdezgubieda M.L. & Barandiaran J.M., (1999), *J. Magn. Magn. Mater.*, **197**,164.

Herzer, G. (1992). *J. Magn. Magn. Mater.* **112**, 258.

Inoue, A., Zhang, T., Koshiba, H., & Makino, A. (1998). *J.Appl.Phys.* **83**,6326.

Idzikowski, B., Baszynski, J., Skorvanek, I., Muller, K.H., & Eckert, D. (1998). *J. Magn. Magn. Materials,* **177-181**,941.

Liu W., Zhang Z.D., Liu J.P., Sun X.K., Zhao X.G. & Cui B.Z., (1999), J. Phys. **32**, 2846.

Sayers, D.E. & Bunker, B. A. (1988). *X-ray Absorption, Principles, Applications, Techniques of EXAFS, SEXAFS and XANES,* edited by Koningsberger, D.,C. & Prins R.,pp.211., New York: John ,Wiley & Sons Inc.

Wan X.H. & Wei S. Q.•(1999). USTCXAFS 1.0 Software Package.

Wu, Z.H., Guo, L., Ju, X., Hu, T.D., Li, Q.S., & Zhu, H.S. (1999).*Chin. Phys. Lett.* **16(8)**, 583.

Wei, S.Q., Liu, W.H., Hu, T.D., Wang, Y.R. & Lu, K.Q. (1998). *Chinese Sic. Bull.* **43,** 396.

Wei ,S.Q., Oyanagi, H., Wen, C.E., Yang ,Y.Z. & Liu, W.H. (1997). *J.Phys:* CM, **9**, 11077.

Wei ,S.Q., Oyanagi, H., Kawanami, H., Sakamoto, K., Sakamoto,T.,& Saini, N.L. (1999). *J. Synchrotron Rad.**6,*** 573-575.

Yoshizawa ,Y., Oguma, S., & Yamauchi, K. (1988). *J.Appl.Phys.* **64**, 6044.